Water Science & Technology

Water Science & Technology Vol 85 No 10, 2928 doi: 10.2166/wst.2022.121

Adsorption of levofloxacin on natural zeolite: effects of ammonia nitrogen and humic acid

Xiaoying Chi[a,b], Lixuan Zeng[a,b,*], Yuejin Du[a,b], Jiaquan Huang[a,b], Yuan Kang[a,b], Jiwen Luo[a,b] and Qiuyun Zhang[a,b]

[a] School of Environment, South China Normal University, 378 Waihuan West Road, Guangzhou 510006, China
[b] Guangdong Provincial Key Laboratory of Chemical Pollution and Environmental Safety and MOE Key Laboratory of Environmental Theoretical Chemistry, Guangzhou, China
*Corresponding author. E-mail: zenglixuan@m.scnu.edu.cn

ABSTRACT

The persistence of antibiotics in sewage treatment plants in recent years has become a serious problem. Meanwhile, humic acid and ammonia nitrogen are widely distributed in natural reservoirs and might influence the sorption, migration and transformation of antibiotics. In this study, natural zeolite (NZ) was evaluated as an adsorbent for the removal of levofloxacin (LEV). The physical and chemical properties of NZ before and after adsorption were characterized by various analytical techniques to develop the mechanism. The effects of ammonia nitrogen and humic acid (HA) on the interfacial behavior of LEV on NZ were explored. Comparative experiments revealed that LEV adsorption on NZ involved electrostatic interactions and ion exchange, and the adsorption processes were well fitted by the Langmuir isotherm model and pseudosecond-order kinetic model. The maximum experimental adsorption capacity of LEV was 22.17 $mg \cdot g^{-1}$ at pH 6.5. The presence of ammonia nitrogen and HA significantly suppressed the adsorption of LEV due to competitive adsorption, and the adsorption capacity decreased 58 and 46%, respectively. It is obvious that low concentrations of ammonia nitrogen and HA are conducive to improving the treatment effect of sewage. This study demonstrates that NZ is a promising and efficient material for LEV adsorption.

Key words: competitive adsorption, electrostatic interaction, ion exchange, levofloxacin, natural zeolite

HIGHLIGHTS

- The adsorption mechanisms are electrostatic interactions and ion exchange mainly.
- Chemical reaction mechanism and intraparticle diffusion mechanism are proposed.
- Ammonia nitrogen leads to cation competition and electrostatic competition.
- Humic acid performs a negative effect on adsorption.

GRAPHICAL ABSTRACT

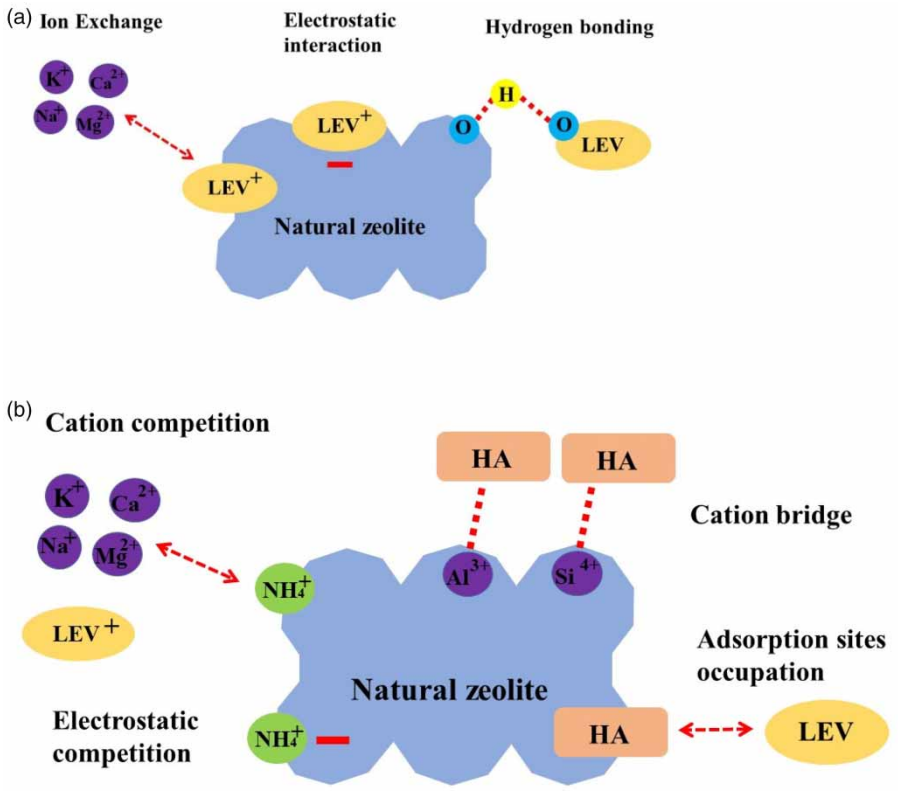

1. INTRODUCTION

Antibiotics have been applied extensively to promote crop production and treat microbial infections in humans and animals. However, up to 80% of antibiotics cannot be metabolized, and they are excreted in their parent form or metabolites through human and animal feces and urine (Ternes 1998). Approximately 46% of various types of antibiotics are ultimately brought into the soil and groundwater through sludge and manure, causing a series of ecological problems and risks to human health (Qiao *et al.* 2018). For example, concentrations of antibiotics in the range of 1.62–575 ng·g^{-1} were detected in agricultural soil of the Huang-Huai-Hai Plain in China, with 24.1% of soil samples exceeding the trigger value of ecotoxicity effects (Pan *et al.* 2021). Furthermore, 12 kinds of antibiotics with total concentrations of 241–1,450 and 69–289 ng·g^{-1} were detected in the estuary and seawater in Laizhou Bay, China (Lu *et al.* 2022). When antibiotics in environmental media accumulate in plant organisms and aquatic organisms, they are likely to be absorbed by humans through the food chain and drinking water.

Levofloxacin (LEV), a third-generation fluoroquinolone antibiotic, is widely applied for the treatment of human and animal bacterial infections. However, it is precisely because of its widespread use that fluoroquinolone exists in a wide range of concentrations in water. A certain amount of fluoroquinolone can be frequently found in wastewater bodies, biosolids and sediments, and its toxicity is released to sustainable ecological development, animal existence and human health (Riaz *et al.* 2018).

At present, two technologies are applied to remove fluoroquinolone from wastewater. Biological treatment, a conventional wastewater treatment, is greatly influenced by various factors, including hydraulic retention time and mixed liquor suspended solids. Clara *et al.* (2005) In addition, the advanced oxidation process is an efficient method for wastewater treatment, but it lacks selectivity and excessively depends on pH (Riaz *et al.* 2018). In addition to these processes, adsorption technology has been successfully applied to the removal of various antibiotics due to its relatively simple design, easy operation, economical cost and efficiency (Figueroa & Mackay 2005; Wang *et al.* 2011).

The adsorption of antibiotics on pure clay minerals, such as montmorillonite (Liu *et al.* 2015) and kaolinite (Li *et al.* 2011; Wu *et al.* 2013), and metal oxides, such as aluminum and iron hydrous oxides (Zhu *et al.* 2020), has been studied by many scholars. Compared with these adsorbents, natural zeolite (NZ) has received attention not only because of its unique adsorption and ion exchange properties but also due to its low market price and relatively simple application and operation (Huang *et al.* 2014). NZ, a crystalline microporous alumina silicate mineral, is a tetrahedron consisting of a three-dimensional structure of Si-O and Al-O through shared oxygen atoms. Due to the alumina silicate surface as the active site for chemical reactions and its use as a molecularly encapsulated cage structure, these properties provide a new research direction for NZ as an adsorbent for various organic substances and heavy metals (Amrhein *et al.* 1996; Chater & Chaouati 2013). The proposed adsorption mechanisms of minerals and antibiotics include cation exchange, cationic bridging, electrostatic attraction and hydrogen bonding (Wang *et al.* 2010).

Natural organic matter, ubiquitous in environmental media, plays an important role in the sorption (Li *et al.* 2019), transport (Engel & Chefetz 2016), and degradation of organic contaminants. Yu *et al.* found that fulvic acid remarkably restricted the antibiotic adsorption process through hydrogen bond interactions (Yu *et al.* 2020). Some humic monomers may enhance antibiotic adsorption and improve antibiotic removal in actual water (Zuo *et al.* 2020). Moreover, with the growth of the population and the development of agriculture and aquaculture, the concentration of ammonia nitrogen in lakes or rivers has increased gradually, which could also affect the migration of antibiotics. The adsorption capacity of NZ for enrofloxacin improved because ammoniated NZ might enhance the ionic interaction (Ötker & Akmehmet-Balcioğlu 2005). Therefore, it is significant to consider the adsorption of antibiotics in the presence of ammonia nitrogen or natural organic matter.

However, to the best of our knowledge, few studies have explored the adsorption mechanism of LEV on NZ and the effect of ammonia nitrogen and natural organic matter on the adsorption. The objectives of the present paper were as follows: (1) The mechanism of LEV adsorption to NZ was elucidated by kinetic models, adsorption isotherms, adsorption thermodynamics and characterization techniques. (2) LEV and ammonia nitrogen were studied separately and jointly to determine their adsorption capacity and competitive adsorption behaviors on NZ. (3) The effect of humic acid (HA), the main component of natural organic matter, on LEV adsorption was evaluated. These findings help to assess the fluidity and fate of LEV in the presence of environmental ammonia nitrogen and HA.

2. MATERIALS AND METHODS

2.1. Chemicals

Levofloxacin solution was prepared by dissolving LEV of analytical grade purchased from Shanghai Macleans of analytical grade, in deionized water. The characteristics and chemical structure of LEV are reported in Table 1. Humic acid and ammonium chloride reagent were of analytical grade. Sodium hydroxide and hydrochloric acid of analytical grade were prepared for pH adjustment. Acetonitrile, methanol and sodium dihydrogen phosphate used to prepare stock solutions were used for chromatographic analysis and were of high-performance liquid chromatography (HPLC) grade. Ultrapure water was used in all procedures without special instructions.

2.2. NZ preparation and characterization

The adsorbent NZ was obtained from Gongyi in Zhejiang. The NZ was sieved to obtain particles with sizes under 100 μm. Next, the NZ particles were cleaned with deionized water to remove any soluble impurities and then dried in an oven at 105 °C for 24 hours. Finally, they were stored in a desiccator to remain dry for future use.

Table 1 | Characteristics and chemical structure of LEV

Structure	Formula	MW (g·mol^{-1})	pK_{a1}	pK_{a2}	Molar volume (cm^3)
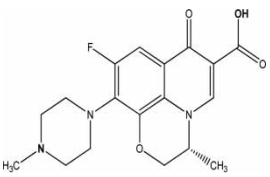	$C_{18}H_{20}FN_3O_4$	361.37	6.05	8.22	278.0 ± 5.0

The surface morphology, elemental composition, crystallinity structure, and surface functional groups of the NZ were characterized. The surface morphology of the NZ was investigated by scanning electron microscopy (SEM, Model Carl Zeiss Ultra 55, Germany). X-ray diffraction analysis (XRD, Utima IV, Japan) and X-ray fluorescence (XRF, Panalytical Axios, Netherlands) were used to analyze the elemental composition and crystalline structure. The Brunauer–Emmett–Teller (BET)-specific surface area, cumulative pore volume, and average pore size distribution for layered double hydroxide (LDH) were determined by the adsorption of N_2 using an automatic surface analyzer (ASAP-2020 Plus, Micrometrics, USA). To explore the adsorption mechanism, LEV-adsorbed NZ and initial NZ were collected and dried in a vacuum oven. A zeta potential analyzer (Zetasizer Nano ZS, UK) was used to measure the potential characteristics of the NZ surface before and after adsorption on LEV. Functional group changes after adsorption were characterized by Fourier transform infrared spectroscopy (FT-IR: Platinum Elmer Spectrum Two, Germany).

2.3. Batch adsorption experiments

The effects of various parameters, including oscillation time, initial LEV concentration, presence of ammonia nitrogen and presence of HA, on LEV removal in batch experiments were studied to explore the adsorption mechanism of LEV on NZ and the influencing factors. A flask containing 100 mL of LEV solution and 0.05 g of NZ was shaken in a 25 °C shaker at a rate of 180 r·min^{-1}. The initial concentration of LEV ranged from 5 mg·L^{-1} to 50 mg·L^{-1}. The supernatant was removed by a syringe at regular intervals after adsorption and then passed through a filter with a 0.45 μm pore size.

The concentration of LEV in the solution was determined by HPLC (Shimadzu LC-16, Suzhou) equipped with a Diamonsil@ Plus 5 C18-A column (Dima, Beijing) at a wavelength of 293 nm. Acetonitrile and 0.025 mol·L^{-1} sodium dihydrogen phosphate solution at a volume ratio of 23:77 were employed as the mobile phase after ultrasonic treatment, and its flow rate was 1 mL·min^{-1}. All samples in the experiment were made into three parallel samples. The amount of LEV adsorbed on NZ was calculated using the following formula:

$$q_e = \frac{(C_0 - C_e)V}{m} \tag{1}$$

where q_e is the amount of LEV adsorbed on NZ (mg·g^{-1}), C_0 is the initial concentration of LEV (mg·L^{-1}), C_e is the concentration of LEV in the solution (mg·L^{-1}) after the reaction, m is the mass of the NZ in the 100 mL solution, and V is the total volume of the reaction solution.

2.3.1. Effect of ammonia nitrogen

LEV solutions (20 mg·L^{-1}) were mixed with ammonia nitrogen concentrations of 10, 20 and 40 mg·L^{-1}, followed by 0.05 g of NZ. The pH values of the mixed solutions were 6.0 and 9.0 with the addition of sodium hydroxide or hydrochloric acid, respectively. The solutions were shaken at a speed of 180 r·min^{-1} in a 25 °C shaker. The supernatant was removed by a syringe at regular intervals, and the concentrations of LEV and ammonia nitrogen were determined. The ammonia nitrogen concentration was determined by using Nessler's reagent spectrophotometric method.

2.3.2. Effect of HA

LEV solutions (20 mg·L^{-1}) were mixed with HA concentrations of 0, 5, 10, 20, 50 and 100 mg·L^{-1}, followed by 0.05 g of NZ. The pH value of the mixed solutions was 6.5 with the addition of sodium hydroxide or hydrochloric acid. The solutions were shaken at a speed of 180 r·min^{-1} in a 25 °C shaker. The supernatant was removed by a syringe at regular intervals, and the concentrations of LEV and HA were determined.

2.4. Adsorption kinetics

The kinetics of the adsorption process are mainly used to describe the rate of adsorption, and the experimental data are fitted by a kinetic model to explain the adsorption mechanism. Classical models commonly used to study adsorption kinetics include the pseudofirst-order kinetic model, pseudosecond-order kinetic model, and intraparticle diffusion model (Khenifi *et al.* 2010).

The pseudofirst-order kinetic, pseudosecond-order kinetic and intraparticle diffusion equations are shown in Equations (2)–(4), respectively:

$$q_t = q_e(1 - e^{-k_1 t}) \tag{2}$$

$$q_t = k_2 q_e^2 t/(1 + k_2 q_e t) \tag{3}$$

$$q_t = K_d t^{1/2} + c \tag{4}$$

where q_e and q_t ($mg{\cdot}g^{-1}$) are the adsorption capacity at equilibrium and time t (min), respectively. k_1 (min^{-1}), k_2 ($g{\cdot}mg^{-1}{\cdot}min^{-1}$) and K_d ($mg{\cdot}g^{-1}{\cdot}min^{-1/2}$) are the rate constants of the pseudofirst-order kinetic, pseudosecond-order kinetic and intraparticle diffusion models, respectively. c is a constant that gives an idea about the boundary layer thickness.

2.5. Adsorption thermodynamics

The concept of adsorption thermodynamics assumes that the entire reaction system is an isolated system whose energy does not disappear or come into being out of thin air. External thermal energy is the power source for the entire system. The Gibbs free energy change is an important criterion for judging whether the adsorption reaction is spontaneous. The thermodynamic formula is as shown in Equations (5) and (6):

$$\Delta G = -RT \ln K \tag{5}$$

$$\ln K = \frac{\Delta S}{R} - \frac{\Delta H}{RT} \tag{6}$$

where K_d is the equilibrium constant ($L{\cdot}g^{-1}$); R is the universal gas constant (8.31 $J{\cdot}mol^{-1}\ K^{-1}$); and T is the temperature (K). The algebraic sum (ΔS) of the entropy change in the reaction process of the system reflects the change in the chaos of the system.

2.6. Adsorption isotherms

Adsorption isotherms contribute to the evaluation of the adsorption capacity of an adsorbent and exploration of the interaction between an adsorbate and adsorbent. The Freundlich and Langmuir equations, two typical isotherm models, are used to describe the adsorption equilibrium process of LEV molecules from wastewater to NZ.

The Langmuir and Freundlich equations are as follows:

$$\frac{C_e}{q_e} = \frac{C_e}{q_m} + \frac{1}{q_m b} \tag{7}$$

$$\ln q_e = \ln k_L + \frac{1}{n} \ln C_e \tag{8}$$

where q_m ($mg{\cdot}g^{-1}$) is the maximum adsorption capacity, K_L ($L{\cdot}mg^{-1}$) and K_F ($mg{\cdot}g^{-1}$) represent the Langmuir and Freundlich constants, respectively, and n is a characteristic constant related to sorption intensity, which gives an indication of how favorable the sorption process is.

A typical isotherm of the obtained experimental data consists of 5–10 points, performed in triplicate.

2.7. NZ regeneration

Adsorption–regeneration cycles were conducted to examine the regeneration efficiency of the zeolite after use.. The adsorbed NZ was collected, and stirred in 1 mol/L NaOH solution at 298 K for 24 h. After desorption, the regenerated NZ was washed with deionized water for several times, and dried in an oven at 100 °C for the next adsorption. The adsorption–regeneration cycles were repeated five times under the condition of 20 $mg{\cdot}L^{-1}$ LEV solution at 298 K.

3. RESULTS AND DISCUSSION

The main objective of this work includes exploring the adsorption mechanism of NZ for antibiotics by kinetic, thermodynamic and isotherm models and the process of adsorbing antibiotics in the presence of ammonia nitrogen and HA.

3.1. Characteristics of adsorbent

NZ was characterized by XRD to determine the mineral structure, and the results are given in Figure 1. The XRD profile of the substrate obtained is typical of the crystalline clinoptilolite phase. The reflections at 2θ of 12.1°, 22.5°, 25.8°, 26.6°, 29.9° and 33.2° correspond to the characteristic reflections of clinoptilolite (Rashid *et al.* 2020). This is consistent with the investigation that NZ comprised clinoptilolite, mainly in other research (Doekhi-Bennani *et al.* 2021; Valdés *et al.* 2021). Clinoptilolite is highly silica-containing and tends to combine with cations because of its negatively charged surface.

The oxide compositions of NZ were determined by XRF analysis, and the results are summarized in Table 2. The samples consist of the main components of silica oxide (SiO_2) and aluminum oxide (Al_2O_3) and other exchangeable cation (K^+, Ca^{2+}, and Fe^{3+}) oxides, potentially being able to be exchanged with other cations, such as ammonium in this study. The different proportions of oxide composition in the NZ depend on geological deposits. The NZ obtained in this study has a higher SiO_2 mass composition than the other NZs previously reported, while the CaO content is reversed. Table 3 shows that NZ consisted of the silicon-rich clinoptilolite with a particularly high Si/Al molar ratio of 17.77. As a hydrophobic and organophilic material, NZ with a high Si/Al ratio is beneficial for wide application in adsorption from water.

The specific surface area of NZ determined by the BET approach was 14.15 $m^2 \cdot g^{-1}$ (Table 4). The pore volume was 0.09 $cm^3 \cdot g^{-1}$, determined by the Barrett–Joyner–Halenda (BJH) methods. The pore size distribution was calculated by applying the

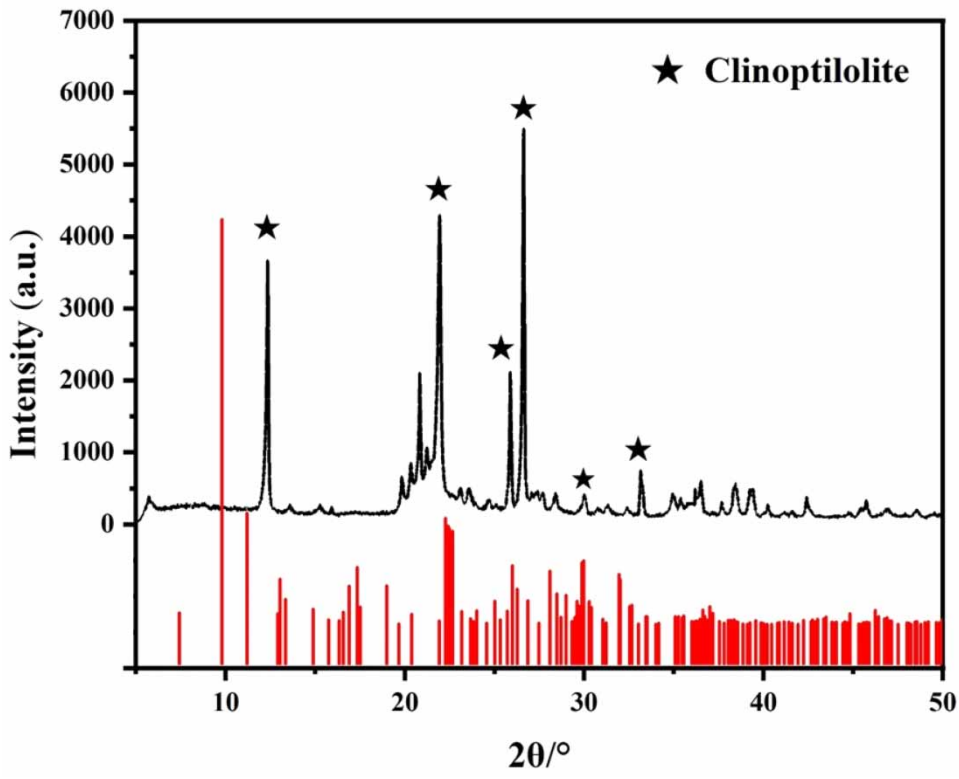

Figure 1 | XRD pattern plot for NZ (red – clinoptilolite-Na).

Table 2 | The oxide composition of NZ before and after adsorption of LEV

	Composition (wt.%)						
	SiO_2	Al_2O_3	Fe_2O_3	Na_2O	K_2O	CaO	MgO
Before adsorption	74.86	20.15	1.44	0.567	1.69	0.341	0.493
After adsorption	76.05	19.76	1.27	0.361	1.58	0.233	0.289

Table 3 | The average chemical composition of NZ by energy dispersive spectroscopy analysis

	Composition (wt.%)						
	O	Si	Al	K	Fe	Ca	Si/Al
Natural zeolite	49.68	43.90	2.47	1.96	1.52	0.13	17.77

Table 4 | Special surface area and pore parameters of NZ

Special surface area ($m^2 \cdot g^{-1}$)	Pore volume ($cm^3 \cdot g^{-1}$)	Average pore size (nm)
14.15	0.09	10.81

cylindrical pore non-local density functional theory (NLDFT) method in the desorption branch (Figure 2). It was observed from Figure 2 that pore diameters are mainly in the 2–4 nm range, which shows that NZ is typical mesoporous material.

Scanning electron microscopy is mainly applied to observe the ultrastructural composition and morphology of the surface of an object. The NZ sample is adhered to a copper table. After surface gold treatment, the morphology and microporous structure of the minerals were analyzed by SEM at an accelerating voltage of 5.00 kV and a vacuum of 10^{-5} Pa. The results are shown in Figure 3, which are SEM images of NZ at different magnifications. It can be seen from the picture that it consists of irregular and coarse aggregates. The platy-shaped crystals correspond to clinoptilolite. It is relatively flat, and many impurities adhere to the surface, presenting a loose sheet structure, which provides favorable channels and pores for the NZ to adsorb pollutants in water.

3.2. Adsorption kinetics

Figure 4 shows that the adsorption rate of NZ toward LEV is divided into two stages: a burst stage and a gentle stage. A burst stage exists from 0 to 15 minutes, in which the adsorption efficiency of NZ toward LEV is greatly increased, and it rises linearly in a short time. A gentle phase is observed from 15–100 min. As the reaction time increases, the adsorption rate decreases gradually, and the reaction equilibrium is close at 100 min. This is because in the initial stage of the process, the surface of the NZ contains a large number of adsorption sites, and the concentration of LEV in the solution is high. The large adsorption and mass transfer driving force enables LEV to be rapidly adsorbed by the NZ in a short time. As the progresses, both the adsorption sites on the surface of the NZ and the concentration of LEV in the solution gradually decrease, resulting in a decrease in the adsorption rate, and the adsorption equilibrium reaches 2 h. The adsorption amount increases with the initial concentration and reaches an adsorption saturation of approximately 20.48 $mg \cdot g^{-1}$ at 20 $mg \cdot L^{-1}$.

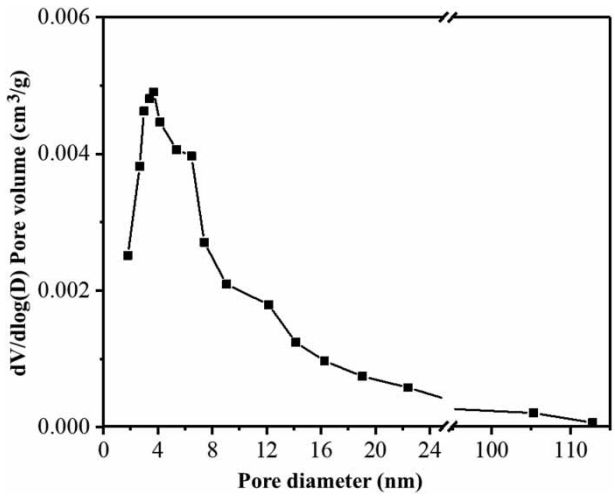

Figure 2 | Pore size distribution of NZ.

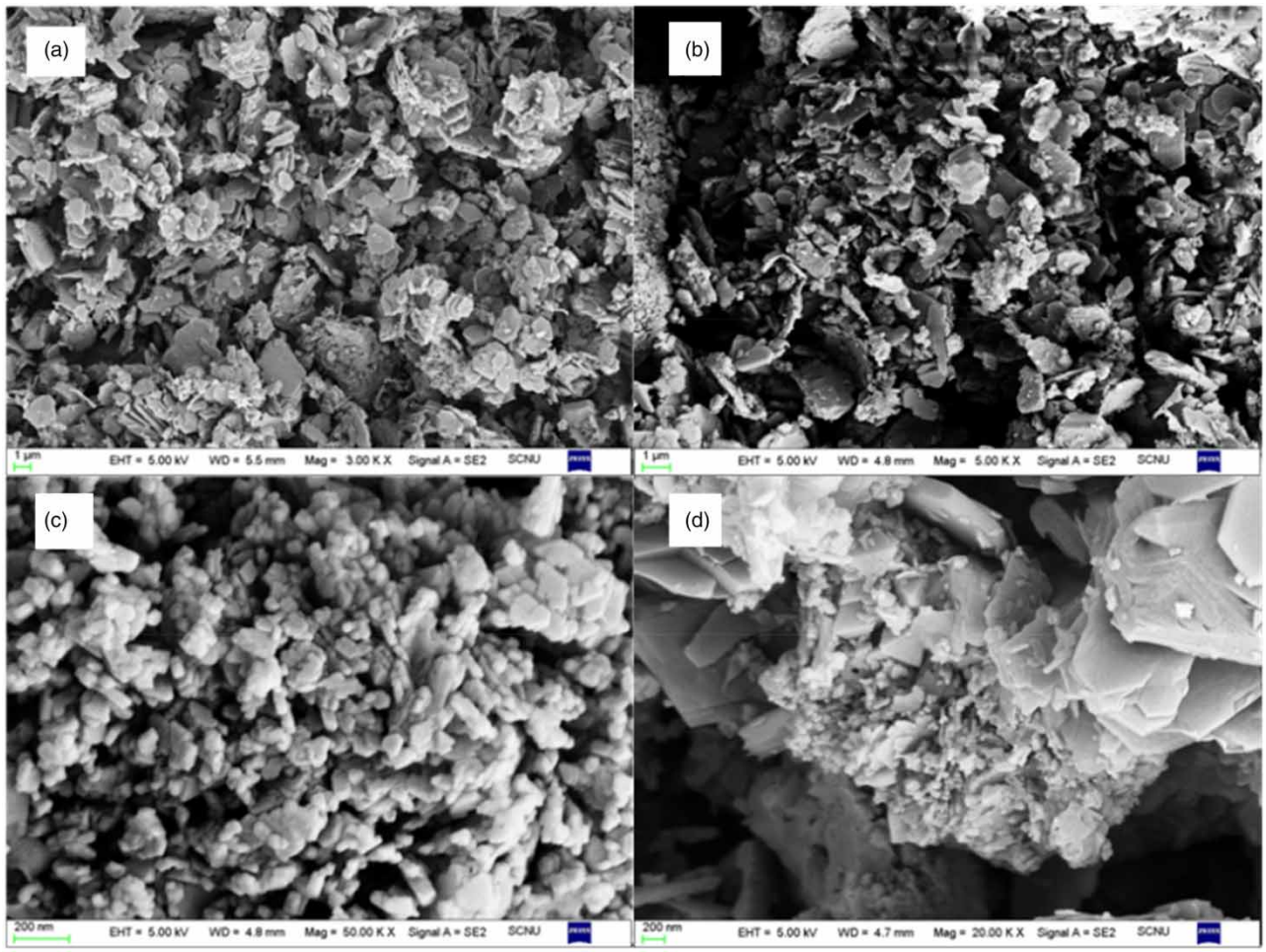

Figure 3 | SEM analysis of NZ.

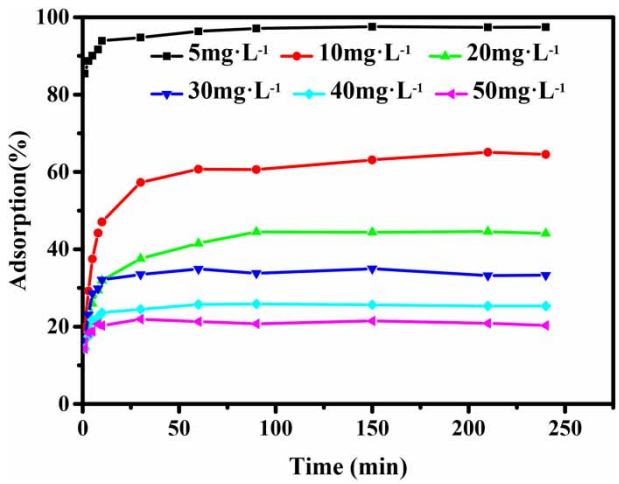

Figure 4 | Effect of adsorption time and initial concentration on LEV removal.

The mechanism of the adsorption process is often dominated by physical and chemical phenomena. Physical phenomena mainly include the mass transfer of the adsorbate in the liquid phase, the diffusion of the liquid phase around the surface of the adsorbent and the diffusion in the pores of the adsorbent. In addition, this chemical phenomenon may involve π–π

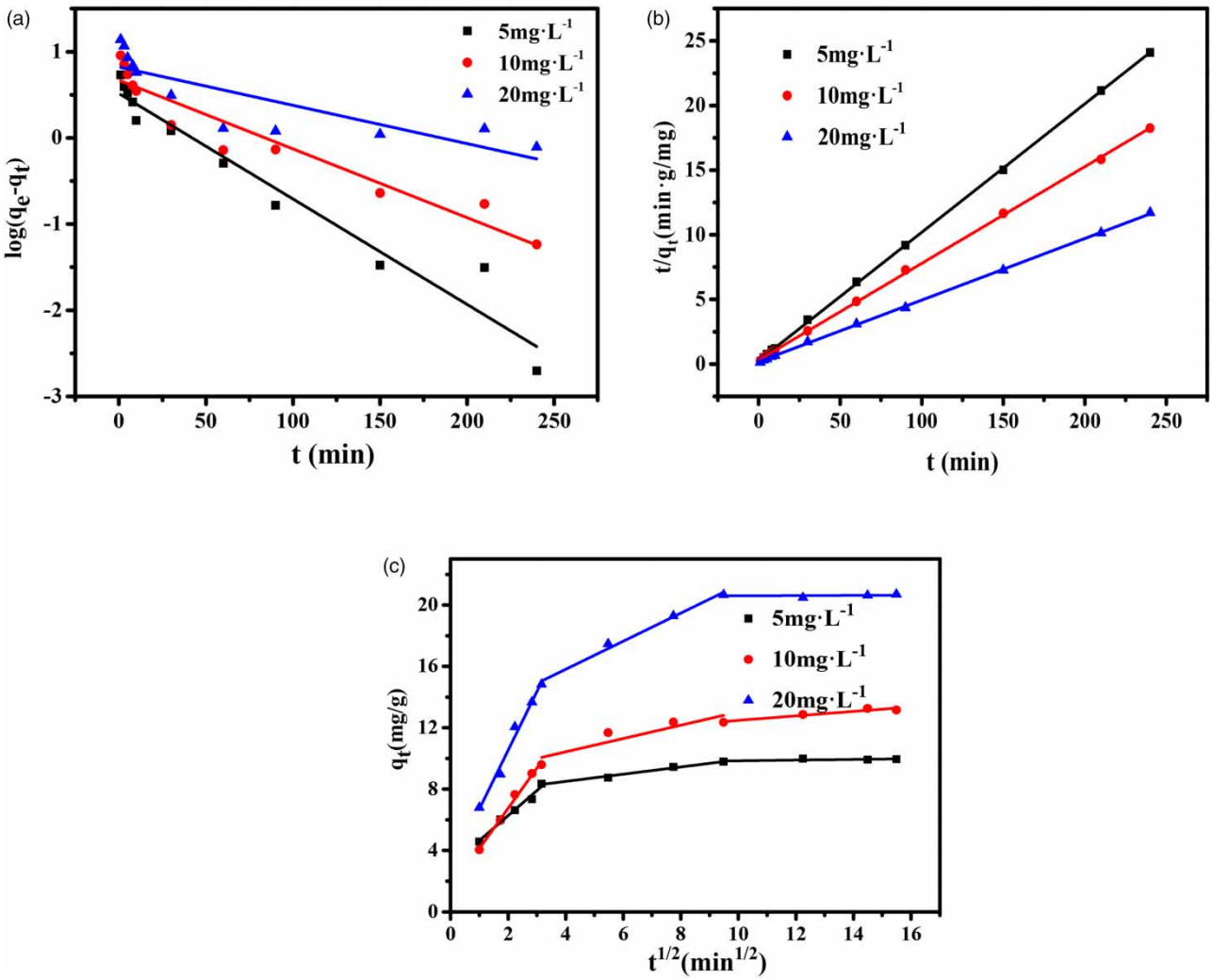

Figure 5 | Pseudofirst-order kinetic model (a), pseudosecond-order kinetic model (b) and intraparticle diffusion model (c) for LEV adsorption onto NZ at different initial LEV concentrations (initial LEV concentration = 5–20 mg·L^{-1}, adsorbent dose = 0.5 g·L^{-1}, pH = 6.5 ± 0.2, shaking speed = 180 r·min^{-1}, temperature = 298 K).

bonding, hydrogen bonding, and electrostatic interactions between the surface active sites of the adsorbent and the adsorbate. The adsorption mechanism can be predicted by analyzing the thermodynamics and kinetics of the adsorption process.

The pseudofirst-order kinetic, pseudosecond-order kinetic and fitted intraparticle diffusion model parameter plots for different LEV concentrations are shown in Figure 5. The results of fitting experimental data with pseudofirst-order, pseudosecond-order and intraparticle diffusion models are shown in Table 5. Based on the correlation coefficient values, it is easy to determine that the pseudosecond-order kinetic model is most suitable for LEV adsorption. The calculated equilibrium adsorption

Table 5 | Kinetic models for LEV adsorption on NZ at 298 K

Pseudofirst-order			Pseudosecond-order			Intraparticle diffusion		
k_1 (min)	q_e (mg·g^{-1})	R^2	k_2 (min)	q_e (mg·g^{-1})	R^2	k_{p1} (mg·g^{-1}·min$^{-1/2}$)	k_{p2} (mg·g^{-1}·min$^{-1/2}$)	k_{p3} (mg·g^{-1}·min$^{-1/2}$)
0.0122	9.96	0.9490	0.0994	9.95	0.9998	1.631	0.2352	0.0230
0.0080	13.21	0.9152	0.0748	13.14	0.9996	2.625	0.4339	0.1456
0.9189	20.91	0.9428	0.0470	20.95	0.9996	3.396	0.8193	0.1208

amount q_e is very close to the experimental value. Therefore, the pseudosecond-order kinetic model can better reflect the adsorption kinetics of NZ on LEV, mainly controlled by chemical reactions related to electron sharing or electron transfer between the adsorbent and adsorbate (Kołodyńska *et al.* 2017; Zhang *et al.* 2017). The fitted particle diffusion rate constant of the particles in the three stages is gradually reduced ($k_{p1} > k_{p2} > k_{p3}$). The first stage has the highest adsorption rate, which represents the migration of LEV ions through the liquid membrane to the surface of the NZ, called membrane diffusion. The second and third linear stages represent the migration of LEV ions through the pores of the outer surface of the NZ into the interior, known as internal diffusion, and the rate of diffusion of contaminants within the particles decreases over time. In addition, it can be seen that the three stages of the fitting equation of the intraparticle diffusion model do not pass through the origin, which indicates that diffusion in the particle is the controlling factor of the rate of the adsorption process. Apart from pore diffusion, there are alternative adsorption mechanisms, such as film diffusion, that accompany it (Xie *et al.* 2015).

3.3. Adsorption thermodynamics

As shown in Table 6, the adsorption of NZ toward LEV exhibits $\Delta G < 0$ and $\Delta H > 0$, indicating that the reaction is a spontaneous heat adsorption process, which is consistent with the study results of adsorption capacity increasing with temperature. ΔS reflects the affinity of the adsorbate to the adsorbent surface, whereas positive entropy indicates that the solvent molecules occupied on the surface are easily displaced by LEV molecules, improving the adsorption capacity. Additionally, $\Delta G < 0$ may illustrate that NZ can be applied to the adsorption of LEV at room temperature.

3.4. Adsorption isotherms

Figure 6 shows the Langmuir and Freundlich plots for LEV adsorption at different temperatures. It was clear that adsorption isotherms at different temperatures could be fitted well using the two isotherm models. The isotherm parameters obtained from the fitting curves to the Langmuir and Freundlich models are given in Table 7. However, the Langmuir model is more suitable than the Freundlich model for describing adsorption isotherms, as reflected by the correlation coefficient

Table 6 | Thermodynamic parameters such as ΔG, ΔH and ΔS for the adsorption of LEV onto NZ

lnT	T (K)	ΔG (kJ·mol^{-1})	ΔS (J·mol^{-1}·K^{-1})	ΔH (kJ·mol^{-1})
0.98	288	−2.34		
1.10	298	−2.73	64.49	16.31
1.42	308	−3.64		

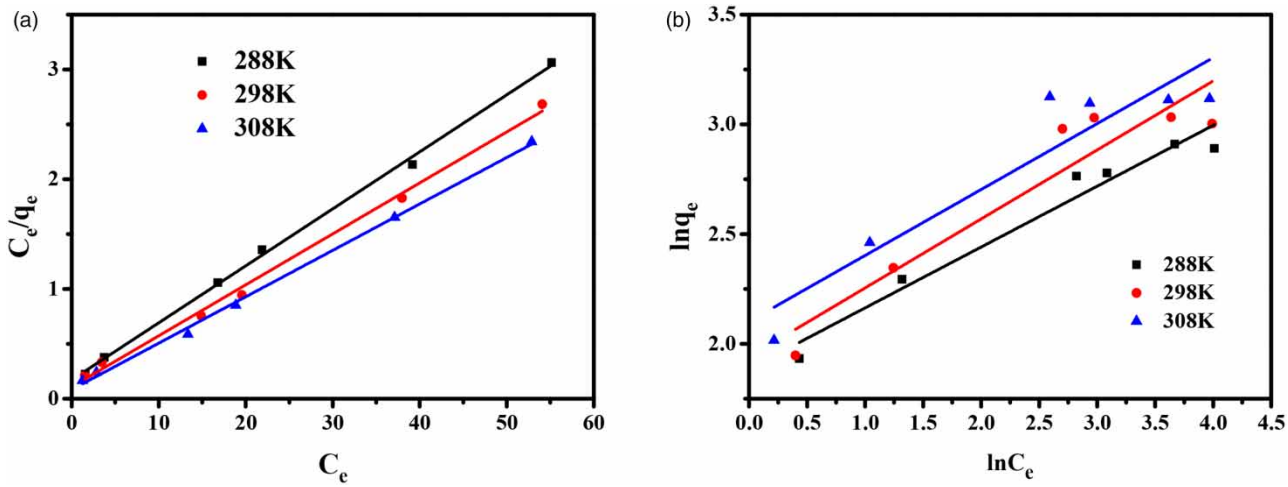

Figure 6 | Langmuir (a) and Freundlich (b) isotherm equations for LEV adsorption onto NZ at different temperatures (initial LEV concentration = 5–50 mg·L^{-1}, adsorbent dose = 0.5 g L^{-1}, pH = 6.5 ± 0.2, shaking speed = 180 r·min^{-1}). Solid lines represent fitting of the data to the Langmuir equation and the Freundlich equation.

Table 7 | Langmuir and Freundlich isotherm parameters and coefficients of determination for the adsorption of LEV onto NZ

	Langmuir			Freundlich		
T (K)	q_m (mg·g^{-1})	K_L (L·mg^{-1})	R^2	K_F (mg·g^{-1})	1/n	R^2
288 K	19.26	0.3010	0.9979	6.5984	0.2772	0.9527
298 K	21.54	0.4251	0.9951	6.9630	0.3143	0.8677
308 K	23.65	0.5061	0.9975	8.1868	0.3003	0.8496

(R^2). The results show that the adsorbent is uniform and that the adsorption film has single layer coverage. Conversely, the maximum single layer adsorption capacity q_m is defined as the total capacity of NZ for LEV adsorption. It increases with an increase in temperature, which indicates that the increase in temperature favors the adsorption of LEV, consistent with the adsorption isotherm analysis. Its maximum value was determined to be 23.65 mg·g^{-1} at 308 K, which may be the reason for the increase in temperature during the reaction and the increase in chemisorption or diffusion (Li *et al.* 2016).

3.5. Proposed adsorption mechanism

In this study, to evaluate the adsorption mechanism of LEV on NZ, Fourier transform infrared (FT-IR) spectroscopy was used. Figure 7 shows the FT-IR spectra of LEV and NZ before and after adsorption of LEV at pH 7. The type of interaction between the functional group of the NZ and the adsorbent LEV was evaluated for changes in peak intensity, peak shift, and peak appearance or disappearance. In general, the characteristic band of NZ is attributed to the vibration of the Si-O-Si bond (950–1,250 cm^{-1}) and the bending and vibration of the hydroxyl group (1,600–1,700 cm^{-1}). At 420–800 cm^{-1}, an adsorption peak is generated by the symmetric stretching vibration of the NZ tetrahedral skeleton structure T-O (T is Si or Al) and the bending vibration of T-O. The strong adsorption peaks at 3,662 and 3,686 cm^{-1} for NZ are ascribed to the stretching vibrations of Si-(OH)-Al and Si-OH, respectively. This verifies that the polar functional groups are on the NZ surface.

The characteristic band of LEV is at 1,000–1,700 cm^{-1}, and the fluctuation of 1,470 cm^{-1} is attributed to the deformation vibration of CH_2 in the piperazine ring. It should be pointed out that this peak at 1,470 cm^{-1} appeared in the spectrum of LEV-loaded NZ, indicating that LEV was successfully adsorbed on NZ. Additionally, the vibration of the adsorption peak at 1,523 cm^{-1} is slightly higher due to the vibration of the N-H group. It is inferred that this is the result of hydrogen bonding between the hydrogen atom of the N-H bond and the oxygen atom on the clay mineral, indicating that the amino group plays an important role in the adsorption process. A stretching vibration peak of adsorbed water or crystal water is generated near 1,637 cm^{-1} (Gomes *et al.* 2017). Furthermore, compared to LEV, LEV-loaded NZ exhibited a loss of the infrared peak at 3,003 cm^{-1}, revealing that the carboxylic group might participate in the interaction.

Figure 8 shows the surface charge of the NZ before and after adsorption in the pH range of 3 to 10. It was found that NZ has a negative surface charge at almost all pH values, which is consistent with that found by others (Nguyen *et al.* 2015;

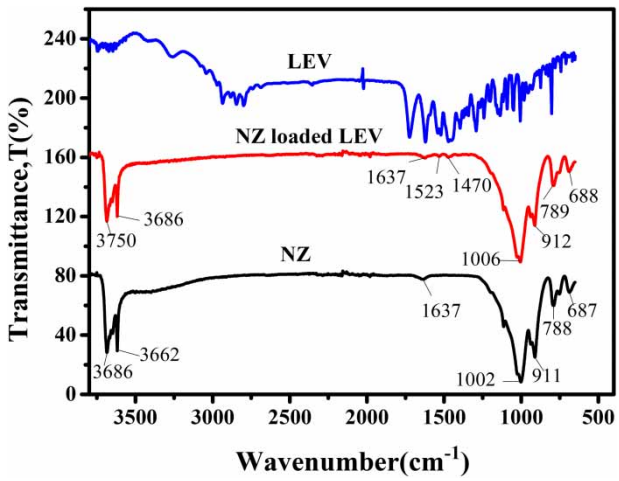

Figure 7 | FT-IR spectra of LEV, NZ, and LEV-loaded NZ.

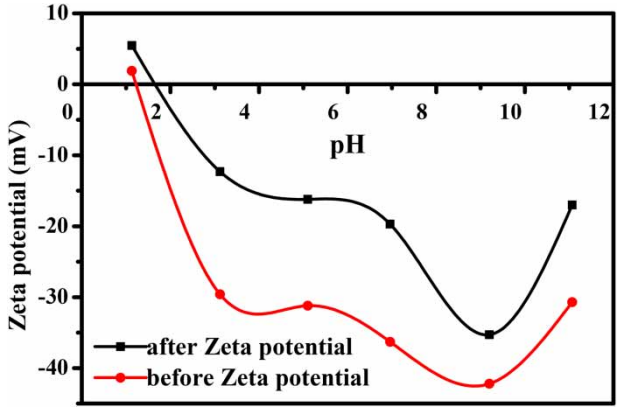

Figure 8 | Zeta potential of NZ before and after adsorption.

Lye *et al.* 2017). This is one of the reasons why NZ is a highly selective adsorbent for cationic contaminants. Under neutral and acidic solution conditions, LEV mainly exists in the form of cationic LEV^+ due to the protonated amino groups in the molecule. After LEV loading, the isoelectric point of NZ moved slightly to a higher pH, indicating that the negative surface of NZ was neutralized by LEV^+ via electrostatic interactions.

Table 2 shows that the proportions of Na^+, K^+, Ca^{2+} and Mg^{2+} decrease after adsorption. This may be explained by that these active cations weakly bind with NZ with platy-shaped crystals, so LEV^+ takes their place. It is highly possible that LEV is taken up by NZ in connection with ion exchange on LEV, which is consistent with the predominant mechanism in the adsorption of ciprofloxacin (Kalebić *et al.* 2021).

3.6. Effect of ammonia nitrogen

For the LEV–ammonia–NZ system, the competitive adsorption of LEV and ammonia nitrogen on NZ is shown in Figure 9. Figure 9(a) shows that the presence of LEV hardly affects the adsorption of ammonia nitrogen by the NZ. It has been proposed that the main mechanism of ammonia nitrogen on NZ is ion exchange (Wang & Peng 2010). In other words, NH_4^+ will exchange with Na^+, K^+, and Ca^{2+} on the surface of NZ. The adsorption amount of NH_4^+ on NZ first increases and then decreases with increasing pH. At low pH, the decrease in ammonia nitrogen removal efficiency was due to the potential competition between NH_4^+ and H^+. Because the radius of NH_4^+ is much larger than that of H^+, NH_4^+ is in a weak position when it competes with H^+ at the exchange position of NZ, which leads to a decrease in the removal rate of NH_4^+. As the pH increases, the H^+ concentration in the wastewater decreases continuously, and NZ can adsorb more NH_4^+. At a pH of 8, the initial concentration was 10 mg·L^{-1}, where the maximum adsorption capacity was 1.45 mg·g^{-1}. When the alkalinity increases, the

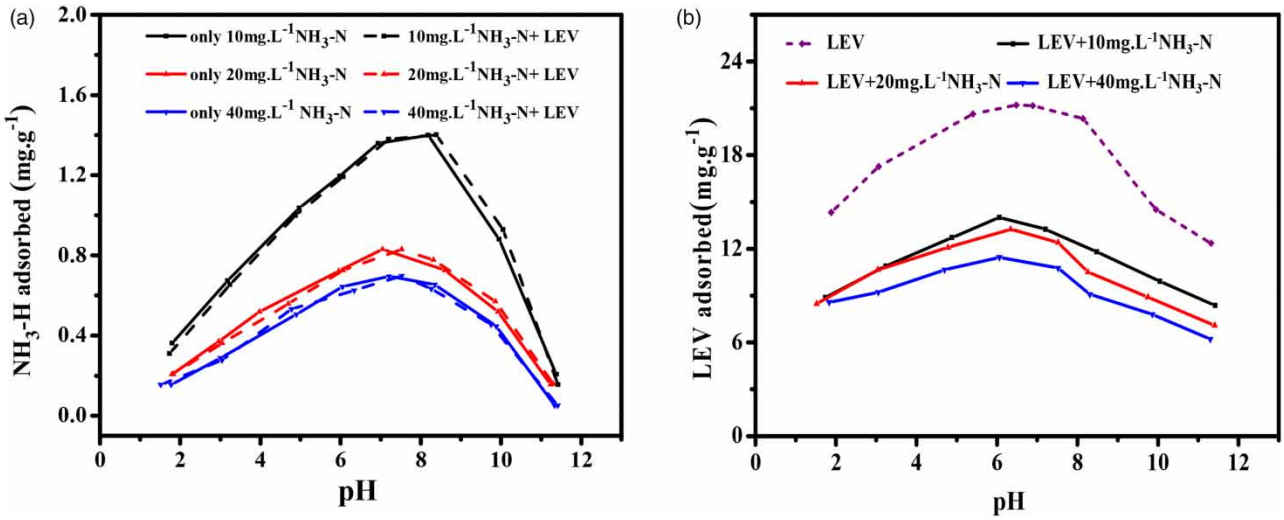

Figure 9 | Competitive adsorption of ammonia nitrogen (a) and 20 mg·L^{-1} LEV (b) on NZ under different pH conditions.

proportion of ammonia in the molecular state increases continuously, which weakens its ion exchange. It mainly relies on the surface adsorption of NZ, so the adsorption amount of ammonia nitrogen decreases.

Conversely, Figure 9(b) shows that the presence of ammonia nitrogen greatly inhibits the adsorption of LEV. At the same time, the inhibition of LEV adsorption by ammonia nitrogen increased with increasing ammonia nitrogen concentration. The maximum adsorption amount of LEV on NZ still appeared at pH 6.5. When the initial concentration was 20 $mg{\cdot}L^{-1}$, the maximum adsorption amount was 22.17 $mg{\cdot}L^{-1}$, which dropped to 10.25 $mg{\cdot}g^{-1}$. The inhibitory effect of ammonia nitrogen on NZ adsorption of LEV may include the following reaction mechanisms: (1) Compared to that of LEV molecules, the radius of NH_4^+ is smaller, and ammonium ions are easily exchanged with the cations on the surface of NZ. In the dual system, it is difficult for LEV to be adsorbed on NZ due to the decrease in the available cations on NZ. (2) Another possibility is electrostatic competition. Under acidic and neutral conditions, both the positively charged amine group in the LEV molecule and the positively charged ammonium ion can bind to the negative surface of NZ. NH_4^+ tends to connect with NZ due to its small radius, so it occupies adsorption sites and prohibits LEV adsorption. Therefore, when NZ is used as the adsorbent to treat low-concentration LEV wastewater, reducing the concentration of ammonia nitrogen is beneficial to improve the treatment effect of LEV.

3.7. Effect of HA

The effect of HA in the range of 0–100 $mg{\cdot}L^{-1}$ on LEV adsorption to NZ at pH 6.5 was investigated by batch experiments. The result is shown in Figure 10, indicating that, as the HA concentration increases, the adsorption capacity of LEV decreases while the adsorption capacity of HA increases. The competitive adsorption may be explained by the following mechanisms: (1) The interaction between HA and NZ may involve cation bridges, since considerable active functional groups such as hydroxyl, carboxylic and amino groups of HA may combine with cations on the NZ surface, such as Al^{3+} and Si^{4+}. (2) Due to their similar functional groups, such as aromatic rings and oxygen- and nitrogen-containing groups, HA may compete with LEV in adsorption and occupy the adsorption sites previously belonging to LEV. (3) Because of the relatively small porosity, HA molecules are generally adsorbed on the exterior surface, while antibiotics can penetrate into the microporous structure (Islam *et al.* 2020). In particular, in neutral and weakly acidic solutions, LEV^+ neutralizes the negative charge of HA, causing an increase in the HA molecule size (Li *et al.* 2019). Therefore, it is likely to block the pore size of NZ and reduce adsorption sites. Qin *et al.* found that hydrophobic interactions and π–π interactions were the major mechanisms for LEV adsorption to natural organic matter (Qin *et al.* 2018), but the influence of these interactions on LEV adsorption to NZ was not found in this study.

3.8. NZ regeneration

Reusability is an important parameter for evaluating the economical applicability of adsorbent. The results of adsorption–regeneration experiments are shown in Figure 11. After three cycles of adsorption and desorption, the regenerated adsorbent still retained good adsorption efficiency. In each cycle, the amount of adsorption decreased by 2–5%, which may be due to the

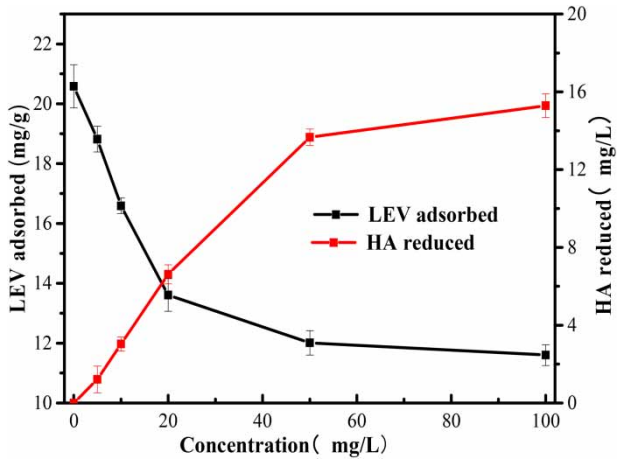

Figure 10 | The effect of HA at different concentrations on adsorption.

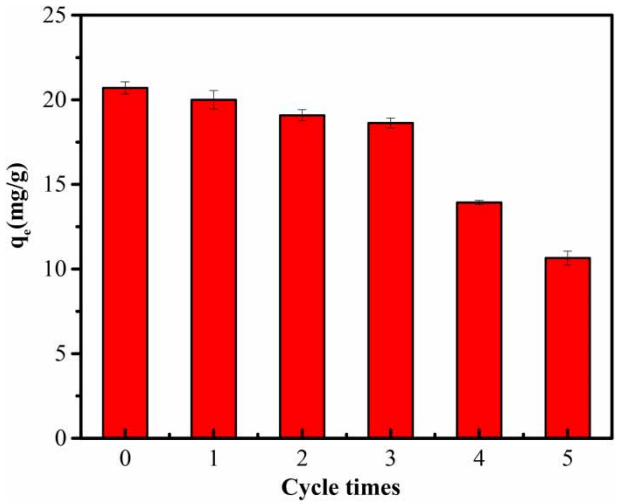

Figure 11 | The experimental results of desorption regeneration of NZ.

loss of irreversible occupation of part of the adsorption sites. However, after the third cycles, the adsorption capacity of NZ particles decreased significantly, and the final adsorption capacity was only 10.65 mg·g^{-1}, which indicated that the adsorbent could be effectively reused three times. The reusability which was observed from other literatures were gathered and compared with this study in Table 8. Lye found that the removal of tetracycline by NZ, the adsorption capacity for tetracycline declined by about 50% after four cycles of regeneration by NaOH solution, which is consistent with this study.

3.9. Comparison of various adsorbents

To evaluate the performance of adsorption of LEV on NZ, adsorption capacities on various adsorbents are presented in Table 9. As observed in Table 9, it showed medium adsorption capacity of NZ. Despite the excellent performance of biochars, they need complex treatment or modification before application and are difficult to be regenerated. Unlike biochars, NZ exists abundantly in nature and is an economical and readily available green adsorbent. Additionally, NZ do not cause secondary pollution after adsorption and exhibits good reusability.

4. CONCLUSION

This study provides insight into the mechanism that accounts for the adsorption of LEV on NZ and explores the influences of ammonia nitrogen and HA. From the results of the present study, the following conclusions can be drawn: (1) The LEV adsorption equilibrium data agree with the Langmuir isotherm model, indicating that this reaction is monolayer adsorption. It was also fit to a pseudosecond-order kinetic model, and the adsorption rate was controlled by the chemical reaction mechanism and the intraparticle diffusion mechanism. The mechanism was dominantly governed by electrostatic interactions and ion exchange. (2) The adsorption capacity of NZ for LEV shows a significant downward trend in the ammonia nitrogen environment due to cation competition and electrostatic competition. The affinity of ammonia nitrogen to NZ is much higher than that of LEV to NZ, which provides a reference for natural mineral treatment of wastewater containing antibiotics.

Table 8 | The comparison of regeneration with other related references

Adsorbent	Adsorbate	Cycle times	Regeneration method	Adsorption capacity reduction	References
MCM-41-zeolite	Tetracycline	5	Ultrasonic vibration in 0.01 M NaOH solution	18.7%	Guo *et al.* (2017)
Natural Clinoptilolite	Ciprofloxacin	4	low-temperature atmospheric pressure plasma treatment	20%	Kalebić *et al.* (2021)
Natural zeolite	Tetracycline	5	0.01 M NaOH solution	50%	Lye *et al.* (2017)
Natural zeolite	Levofloxacin	5	1 M NaOH solution	52%	This work

Table 9 | The comparison of LEV adsorption capacity between different adsorbents

Adsorbent	LEV initial concentration ($mg \cdot L^{-1}$)	Adsorption capacity ($mg \cdot g^{-1}$)	References
Goethite	0.04–0.08	0.78	Qin *et al.* (2014)
Coconut coir charcoal with Al_2O_3 nanoparticles	0.7–5.0	1.80	Limbikai *et al.* (2016)
Rice-husk biochars	40–75	4.99	Yi *et al.* (2016)
Magnetic nanoparticles	2.5–20	6.848	Eniola *et al.* (2019)
Wood chip biochars	50–150	7.72	Yi *et al.* (2016)
Mechanochemistry-treated zeolite	5.5–67	47.68	Chen *et al.* (2019)
Iron-pillared montmorillonite	20–100	48.61	Liu *et al.* (2015)
Rectorite	20–100	63.38	Feng *et al.* (2019)
Chitosan/biochar hydrogel beads	5–160	76	Afzal *et al.* (2018)
Natural zeolite	5–50	22.17	This work

(3) Around the pH of natural bodies of water, HA has a negative effect on LEV adsorption to NZ, as HA preferentially interacts with NZ and shields the surface adsorption sites. (4) NZ is recyclable and retained good adsorption efficiency after three rounds of sorption-desorption cycles.

In summary, when NZ is used as the adsorbent to treat low-concentration LEV wastewater, reducing the concentration of ammonia nitrogen and HA is beneficial to improving the treatment effect of LEV.

ACKNOWLEDGEMENTS

This work was supported by Major Science and Technology Program for Water Pollution Control and Treatment (2017ZX07202004) and the Science and Technology Plan Project of Guangzhou (201510010006). In addition, the linguistic of this manuscript was assisted by the premium editing of American Journal Experts.

DATA AVAILABILITY STATEMENT

All relevant data are included in the paper or its Supplementary Information.

REFERENCES

Afzal, M. Z., Sun, X. F., Liu, J., Song, C., Wang, S. G. & Javed, A. 2018 Enhancement of ciprofloxacin sorption on chitosan/biochar hydrogel beads. *Science of the Total Environment* **639**, 560–69. https://doi.org/10.1016/j.scitotenv.2018.05.129.

Amrhein, C., Haghnia, G. H., Kim, T. S., Mosher, P. A., Gagajena, R. C., Amanios, T. & de la Torre, L. 1996 Synthesis and properties of zeolites from coal fly ash. *Environmental Science and Technology* **30** (3), 735–742.

Chater, M. & Chaouati, N. 2013 Adsorption of phenol from aqueous solution onto zeolites Y modified by silylation. *Comptes Rendus Chimie* **16**, 222–228. https://doi.org/10.1016/j.crci.2012.10.010.

Chen, Z., Ma, W., Lu, G., Meng, F., Duan, S., Zhang, Z., Wei, L. & Pan, Y. 2019 Adsorption of levofloxacin onto mechanochemistry treated zeolite: modeling and site energy distribution analysis. *Separation and Purification Technology* **222**, 30–34. https://doi.org/10.1016/j.seppur.2019.04.010.

Clara, M., Kreuzinger, N., Strenn, B., Gans, O. & Kroiss, H. 2005 The solids retention time – A suitable design parameter to evaluate the capacity of wastewater treatment plants to remove micropollutants. *Water Research* **39** (1), 97–106. https://doi.org/10.1016/j.watres.2004.08.036.

Doekhi-Bennani, Y., Leilabady, N. M., Fu, M., Rietveld, L. C., van der Hoek, J. P. & Heijman, S. G. J. 2021 Simultaneous removal of ammonium ions and sulfamethoxazole by ozone regenerated high silica zeolites. *Water Research* **188**, 116472. https://doi.org/10.1016/j.watres.2020.116472.

Engel, M. & Chefetz, B. 2016 Removal of triazine-based pollutants from water by carbon nanotubes: impact of dissolved organic matter (DOM) and solution chemistry. *Water Research* **106**, 146–154. https://doi.org/10.1016/j.watres.2016.09.051.

Eniola, J. O., Kumar, R. & Barakat, M. A. 2019 Adsorptive removal of antibiotics from water over natural and modified adsorbents. *Environmental Science and Pollution Research* **26** (34), 34775–34788. https://doi.org/10.1007/s11356-019-06641-6.

Feng, Y., Lixuan, Z., Jiwen, L. U. O., Qiuyun, Z. & Yuan, K. 2019 The adsorption of levofloxacin onto rectorite. *Journal of South China Normal University (Natural Science Edition)* **51** (1), 56–62.

Figueroa, R. A. & Mackay, A. A. 2005 Sorption of oxytetracycline to iron oxides and iron oxide-rich soils. *Environmental Science and Technology* **39** (17), 6664–6671.

Gomes, G. J., Zalzar, M. F., Lindino, C. A., Scremin, F. R., Bittencourt, P. R. S., Costa, M. B. & Peruchena, N. M. 2017 Adsorption of acetic acid and methanol on H-Beta zeolite: an experimental and theoretical study. *Microporous and Mesoporous Materials* **252**, 17–28. https://doi.org/10.1016/j.micromeso.2017.06.008.

Guo, Y., Huang, W., Chen, B., Zhao, Y., Liu, D., Sun, Y. & Gong, B. 2017 Removal of tetracycline from aqueous solution by MCM-41-Zeolite A loaded nano zero valent iron: synthesis, characteristic, adsorption performance and mechanism. *Journal of Hazardous Materials* **339**, 22–32. https://doi.org/10.1016/j.jhazmat.2017.06.006.

Huang, H., Xiao, D., Pang, R., Han, C. & Ding, L. 2014 Simultaneous removal of nutrients from simulated swine wastewater by adsorption of modified zeolite combined with struvite crystallization. *Chemical Engineering Journal* **256**, 431–438. https://doi.org/10.1016/j.cej.2014.07.023.

Islam, M. A., Morton, D. W., Johnson, B. B. & Angove, M. J. 2020 Adsorption of humic and fulvic acids onto a range of adsorbents in aqueous systems, and their effect on the adsorption of other species: a review. *Separation and Purification Technology* **247**, 116949. https://doi.org/10.1016/j.seppur.2020.116949.

Kalebić, B., Pavlović, J., Dikić, J., Rečnik, A., Gyergyek, S., Škoro, N. & Rajić, N. 2021 Use of natural clinoptilolite in the preparation of an efficient adsorbent for ciprofloxacin removal from aqueous media. *Minerals* **11** (5). https://doi.org/10.3390/min11050518.

Khenifi, A., Derriche, Z., Mousty, C., Prévot, V. & Forano, C. 2010 Adsorption of glyphosate and glufosinate by Ni_2AlNO_3 layered double hydroxide. *Applied Clay Science* **47** (3–4), 362–371. https://doi.org/10.1016/j.clay.2009.11.055.

Kołodyńska, D., Hałas, P., Franus, M. & Hubicki, Z. 2017 Zeolite properties improvement by chitosan modification – sorption studies. *Journal of Industrial and Engineering Chemistry* **52**, 187–196. https://doi.org/10.1016/j.jiec.2017.03.043.

Li, W., Zeng, L., Kang, Y., Zhang, Q., Luo, J. & Guo, X. 2016 A solid waste, crashed autoclaved aerated concrete, as a crystalline nucleus for the removal of low concentration of phosphate. *Desalination and Water Treatment* **57** (30), 14169–14177. https://doi.org/10.1080/19443994.2015.1062432.

Li, Y., Bi, E. & Chen, H. 2019 Effects of dissolved humic acid on fluoroquinolones sorption and retention to kaolinite. *Ecotoxicology and Environmental Safety* **178**, 43–50. https://doi.org/10.1016/j.ecoenv.2019.04.002.

Limbikai, S. S., Deshpande, N. A., Kulkarni, R. M., Khan, A. A. P. & Khan, A. 2016 Kinetics and adsorption studies on the removal of levofloxacin using coconut. *Desalination and Water Treatment* **57** (50), 23918–23926.

Li, Z., Hong, H., Liao, L., Ackley, C. J., Schulz, L. A., MacDonald, R. A., Mihelich, A. L. & Emard, S. M. 2011 A mechanistic study of ciprofloxacin removal by kaolinite. *Colloids and surfaces. B, Biointerfaces* **88** (1), 339–344. https://doi.org/10.1016/j.colsurfb.2011.07.011.

Liu, Y., Dong, C., Wei, H., Yuan, W. & Li, K. 2015 Adsorption of levofloxacin onto an iron-pillared montmorillonite (clay mineral): kinetics, equilibrium and mechanism. *Applied Clay Science* **118**, 301–307. https://doi.org/10.1016/j.clay.2015.10.010.

Lu, S., Lin, C., Lei, K., Xin, M., Gu, X., Lian, M., Wang, B., Liu, X., Ouyang, W. & He, M. 2022 Profiling of the spatiotemporal distribution, risks, and prioritization of antibiotics in the waters of Laizhou Bay, northern China. *Journal of Hazardous Materials* **424**, 127487. https://doi.org/10.1016/j.jhazmat.2021.127487.

Lye, J. W. P., Saman, N., Sharuddin, S. S. N., Othman, N. S., Mohtar, S. S., Noor, A. M. M., Buhari, J., Cheu, S. C., Kong, H. & Mat, H. 2017 Removal performance of tetracycline and oxytetracycline from aqueous solution via natural zeolites: an equilibrium and kinetic study. *CLEAN – Soil, Air, Water* **45** (10). https://doi.org/10.1002/clen.201600260.

Nguyen, T. C., Loganathan, P., Nguyen, T. V., Vigneswaran, S., Kandasamy, J. & Naidu, R. 2015 Simultaneous adsorption of Cd, Cr, Cu, Pb, and Zn by an iron-coated Australian zeolite in batch and fixed-bed column studies. *Chemical Engineering Journal* **270**, 393–404. https://doi.org/10.1016/j.cej.2015.02.047.

Ötker, H. M. & Akmehmet-Balcioğlu, I. 2005 Adsorption and degradation of enrofloxacin, a veterinary antibiotic on natural zeolite. *Journal of Hazardous Materials* **122** (3), 251–258. https://doi.org/10.1016/j.jhazmat.2005.03.005.

Pan, Z., Yang, S., Zhao, L., Li, X., Weng, L., Sun, Y. & Li, Y. 2021 Temporal and spatial variability of antibiotics in agricultural soils from. *Chemosphere* **272**, 129803. https://doi.org/10.1016/j.chemosphere.2021.129803.

Qiao, M., Ying, G. G., Singer, A. C. & Zhu, Y. G. 2018 Review of antibiotic resistance in China and its environment. *Environment International* **110**, 160–172. https://doi.org/10.1016/j.envint.2017.10.016.

Qin, X., Liu, F., Wang, G., Weng, L. & Li, L. 2014 Adsorption of levofloxacin onto goethite: effects of pH, calcium and phosphate. *Colloids and Surfaces B. Biointerfaces* **116**, 591–596. https://doi.org/10.1016/j.colsurfb.2013.09.056.

Qin, X., Du, P., Chen, J., Liu, F., Wang, G. & Weng, L. 2018 Effects of natural organic matter with different properties on levofloxacin adsorption to goethite: experiments and modeling. *Chemical Engineering Journal* **345**, 425–431. https://doi.org/10.1016/j.cej.2018.03.125.

Rashid, T., Iqbal, D., Hazafa, A., Hussain, S., Sher, F. & Sher, F. 2020 Formulation of zeolite supported nano-metallic catalyst and applications in textile effluent treatment. *Journal of Environmental Chemical Engineering* **8** (4), 104023. https://doi.org/10.1016/j.jece.2020.104023.

Riaz, L., Mahmood, T., Khalid, A., Rashid, A., Siddique, M. B. A., Kamal, A. & Coyne, M. S. 2018 Fluoroquinolones (FQs) in the environment: a review on their abundance, sorption and toxicity in soil. *Chemosphere* **191**, 704–720. https://doi.org/10.1016/j.chemosphere.2017.10.092.

Ternes, T. A. 1998 Occurrence of drugs in German sewage treatment plants and rivers. *Water Research* **32** (11), 3245–3260. https://doi.org/10.1016/S0043-1354(98)00099-2.

Valdés, H., Riquelme, A. L., Solar, V. A., Azzolina-Jury, F. & Thibault-Starzyk, F. 2021 Removal of chlorinated volatile organic compounds onto natural and Cu-modified zeolite: the role of chemical surface characteristics in the adsorption mechanism. *Separation and Purification Technology* **258**. https://doi.org/10.1016/j.seppur.2020.118080.

Wang, S. & Peng, Y. 2010 Natural zeolites as effective adsorbents in water and wastewater treatment. *Chemical Engineering Journal* **156** (1), 11–24. https://doi.org/10.1016/j.cej.2009.10.029.

Wang, C.-J., Li, Z., Jiang, W.-T., Jean, J.-S. & Liu, C.-C. 2010 Cation exchange interaction between antibiotic ciprofloxacin and montmorillonite. *Journal of Hazardous Materials* **183** (1–3), 309–314. https://doi.org/10.1016/j.jhazmat.2010.07.025.

Wang, C.-J., Li, Z. & Jiang, W.-T. 2011 Adsorption of ciprofloxacin on 2:1 dioctahedral clay minerals. *Applied Clay Science* **53** (4), 723–728. https://doi.org/10.1016/j.clay.2011.06.014.

Wu, Q., Li, Z. & Hong, H. 2013 Adsorption of the quinolone antibiotic nalidixic acid onto montmorillonite and kaolinite. *Applied Clay Science* **74**, 66–73. https://doi.org/10.1016/j.clay.2012.09.026.

Xie, M., Zeng, L., Zhang, Q., Kang, Y., Xiao, H., Peng, Y., Chen, X. & Luo, J. 2015 Synthesis and adsorption behavior of magnetic microspheres based on chitosan/organic rectorite for low-concentration heavy metal removal. *Journal of Alloys and Compounds* **647**, 892–905. https://doi.org/10.1016/j.jallcom.2015.06.065.

Yi, S., Gao, B., Sun, Y., Wu, J., Shi, X., Wu, B. & Hu, X. 2016 Removal of levofloxacin from aqueous solution using rice-husk and wood-chip biochars. *Chemosphere* **150**, 694–701. https://doi.org/10.1016/j.chemosphere.2015.12.112.

Yu, F., Li, Y., Huang, G., Yang, C., Chen, C. & Zhou, T. 2020 Adsorption behavior of the antibiotic levofloxacin on microplastics in the presence of different heavy metals in an aqueous solution. *Chemosphere* **260**, 127650. https://doi.org/10.1016/j.chemosphere.2020.127650.

Zhang, Y., Zeng, L., Kang, Y., Luo, J., Li, W. & Zhang, Q. 2017 Sustainable use of autoclaved aerated concrete waste to remove low concentration of Cd(II) ions in wastewater. *Desalination and Water Treatment* **82**, 170–178. https://doi.org/10.5004/dwt.2017.20909.

Zhu, Y., Yang, Q., Lu, T., Qi, W., Zhang, H., Wang, M., Qi, Z. & Chen, W. 2020 Ecotoxicology and environmental safety effect of phosphate on the adsorption of antibiotics onto iron oxide minerals: comparison between tetracycline and ciprofloxacin. *Ecotoxicology and Environmental Safety* **205**, 111345. https://doi.org/10.1016/j.ecoenv.2020.111345.

Zuo, X., Qian, C., Ma, S. & Xiong, J. 2020 Sulfonamide antibiotics sorption by high silica ZSM-5: effect of pH and humic monomers (vanillin and caffeic acid). *Chemosphere* **248**, 126061. https://doi.org/10.1016/j.chemosphere.2020.126061.

First received 16 February 2022; accepted in revised form 29 March 2022. Available online 11 April 2022